Physics Informed Gated Recurrent Unit Networks for Li-ion Battery State Estimation

Vishnu Ram Jawaharram Yashaswini Inala Zarin Musarrat Manita
Arizona State University
Tempe, AZ, USA
{vjawahar, yinala, zmanita}@asu.edu

Abstract

Currently, the mobility and Grid energy storage platforms rely heavily on lithium-ion (Li-ion) batteries as their primary source of storage, transitioning from fossil fuel-based energy. Due to the increasing demand for Li-ion batteries. The Battery Management System (BMS), as an embedded device, is essential for ensuring both the user's safety and the protection of the battery. While the BMS performs various protection and estimation tasks, it also accurately estimates the Li-ion battery's state of charge (SOC) and state of health (SOH) when required. The conventional methods for estimation include Equivalent Circuit Model (ECM), Open Circuit Voltage (OCV) with a SOC curve-based direct look-up method, and a Kalman filter-based estimation method. The more recent advances include the data-driven method, which uses various ML algorithms. The conventional methods fail to generalize over varying operating conditions, and the data-driven method often lacks the physical interpretation of the actual system.

This paper proposes a Novel Physics-Informed Gated Recurrent Unit network (GRU-PINN) for estimation of both the SOC and SOH estimation of Li-ion batteries. The proposed model integrates battery electrochemical principles – Coulomb Counting dynamics for SOC and Differential Voltage Analysis (DVA) behavior for SOH – directly into the neural network loss function. Three architectures – LSTM, GRU, and GRU-PINN – are evaluated for both SOC and SOH estimation using the Oxford battery dataset.

Our results show that for SOH estimation, the GRU model achieves the best performance, outperforming both LSTM and GRU-PINN, with an error of $MAE = 0.127\%$, $RMSE = 0.154\%$, and Max Error $= 0.539\%$. For SOC estimation, the GRU-PINN significantly improves mid-range SOC prediction after physics-based augmentation, achieving $MAE = 0.173\%$, $RMSE = 0.219\%$, and Max Error $= 1.0557\%$, outperforming traditional LSTM and GRU baselines. The proposed pipeline demonstrates strong robustness to sensor noise and offers a lightweight architecture suitable for real-time embedded BMS deployment. These findings show that selective physics integration enhances SOC estimation accuracy while a pure GRU model suffices for reliable SOH estimation.

1. Introduction

Li-ion batteries have become one of the most preferred energy storage solutions for both consumer electronic systems and large-scale power applications due to their high energy density, power density, long shelf life, and lack of memory effect [1]. SOC and SOH estimation are among the primary algorithmic features of the BMS. SOC represents the current capacity of the cell that can be discharged under specific battery conditions, such as temperature, and ensures the battery remains safe, typically expressed as a percentage. Although SOC and SOH cannot be measured directly by means of any temperature, it has to be estimated from the measurable quantities such as the voltage, temperature, and current. As shown in Equation 1, the State of Charge (SOC) is calculated as the ratio of the remaining to the rated capacity [2].

$$SOC(\%) = \frac{Q_{\text{remaining}}}{Q_{\text{rated}}} \times 100 \tag{1}$$

In the above equation, $Q_{\text{remaining}}$ represents the remaining charge in the battery in Ampere-hours (*Ah*), and Q_{rated} denotes the rated nominal capacity of the battery in *Ah*.

SOH is the estimated quantity of the degradation level with respect to the beginning of life. The degradation is due to loss of usable energy or power, which leads to a decrease in the range and acceleration when we consider the case of a battery electric vehicle (BEV). Also loss of capacity in both energy storage and BEV. The degradation of the Li-ion Battery can be categorized into three different categories. Loss of lithium inventory (LLI) when lithium ions are no longer available for intercalation or deintercalation as a result of some side reaction, Loss of active material of the anode (LAMA) caused by particle cracking and loss of electrical contact or the solid surface blocks the active areas, and Loss of active material of the cathode (LAMC) caused due to structural failure, particle cracking or loss of electrical contact [3]. The formula used to calculate SOH in percentage is shown in 2.

$$SOH(\%) = \frac{Q_{\text{current}}}{Q_{\text{rated}}} \times 100 \quad (2)$$

In the above equation, Q_{current} represents the maximum current capacity of the Battery, and Q_{rated} denotes the rated nominal capacity of the battery in *Ah* at the beginning of life (BOL). Estimating these parameters is also challenging due to the dependency between them. Accurate estimation of SOC requires knowledge of the current SOH, while the SOH estimation benefits from the SOC accuracy over complete charge and discharge cycles. Particularly, the SOC estimation of the Li-ion cell with Lithium Ferrous Phosphate (LFP) chemistry is challenging, given the flat charge and discharge curves.

There are three categories in which the SOC is estimated: the AH integration method, also known as Coulomb Counting (CC), which calculates the charge by integrating the current, and is prone to inaccuracies due to sensor readings and the initial calibration of the battery's SOC. The formula to calculate the SOC using the CC method is given in 3.

$$SOC(\%) = SOC(t_0)(\%) - \frac{100 * \eta}{Q_{\text{rated}}} \int_{t_0}^{t} I(\tau)\, d\tau \quad (3)$$

In Equation 3, $SOC(t_0)$ represents the initial state of charge obtained from the open-circuit voltage (OCV) versus SOC calibration curve, which serves as the reference point for the coulomb counting method. The term Q_{rated} denotes the rated capacity of the battery, measured in *Ah*. Two different methods, the model-based approach, which depends on the Equivalent Circuit(ECM) Model, and the data-driven method, were explored further in order to avoid the inaccuracies in measurement to an extent. Model-based approaches like the Extended Kalman Filter (EKF), the Unscented Kalman Filter (UKF), and the Model Predictive Control (MPC) give more accurate results, incorporating battery dynamics from ECM [4], [5], [6].

The data-driven methods, particularly deep learning architectures such as the Long Short-Term Memory (LSTM) and Gated Recurrent Unit (GRU) networks, demonstrate a higher order of accuracy by learning the temporal dependencies directly from the charge and discharge data, where the cell goes into various tests, such a charging, discharging, and impedance testing. While these methods provide impressive accuracy, they lack physics interpretability in the training process, and there is no predictive strategy for the battery dynamics for various battery chemistries. Additionally, the data generation process is time-consuming, particularly for SOH estimation, which requires a long-term dataset spanning several months to years. It is also observed that many data-driven algorithms, although they produce promising results, do not consider the joint estimation of both parameters; instead, they predict just one of these two parameters, which is incorrect, given that both parameters are interdependent.

This article introduces the Physics-Informed Neural Network (PINN) applied for the estimation of both SOC and SOH separately, specifically by developing a physics-informed Gated Recurrent Unit architecture. The novelty in this approach lies in incorporating physical constraints, such as the ECM model dynamics and the capacity fade principle, as components in the actual loss function of the GRU architecture. The proposed architecture offers several advantages over existing frameworks, particularly in reducing the data required for training, which is especially beneficial for SOH estimation. Using the GRU over the LSTM network gives the model a competitive edge in terms of computational efficiency and increased accuracy, making it ideal for real-time deployment in actual hardware.

2. Related Work

The battery SOC and SOH estimation can be performed in various approaches; a few of them are shown in Fig.1.

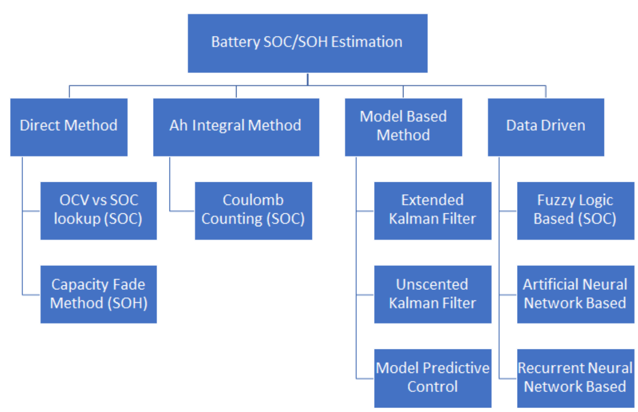

Figure 1. SOC and SOH estimation methods

Direct Method

A paper by Piller *et al.* discusses the Direct method of SOC estimation called the OCV-SOC lookup method. Under no-load or rest conditions, the terminal voltage approximates the true open-circuit voltage (OCV) of the battery, allowing the SOC to be directly inferred from a pre-calibrated OCV–SOC curve or lookup table [7]. Although this is simple, it requires a significant amount of time to obtain the actual OCV of the battery. This curve also varies with temperature, aging, and cell chemistry – all of which increase the possibility of inaccurate SOC estimation.

Conversely, the capacity fade method of determining the SOH of the battery is discussed in [8] and [9]. SOH is estimated by charging and discharging the cell and comparing the current capacity to its capacity at the Beginning of Life (BOL). This method does not capture the effects of power degradation and provides an incomplete picture of the battery's SOH.

These papers expand on one of the main drawbacks of these direct methods – they cannot be used online as a hardware feature, so most of the current BMS do not have this kind of estimation feature.

Ah Integral Method

The Coulomb counting method is the current-based approach [10] which computes the amount of Coulombs added/removed from the battery in order to compute the SOC as a ratio between the remaining Coulombs and the battery capacity that is assumed known. However, the main error in this approach [11] arises from the uncertainty in the above assumption. A current measurement error also exists because sensors are usually corrupted by measurement noise. As small inaccuracies in measurement add up over time, it leads to significant SOC drift. Current sensor offset, bias, and quantization noise also directly affect SOC estimation accuracy.

Model Based Methods

Acquarone et al. explored the extended Kalman filter method for SOC and SOH estimation in electric vehicle applications. The extended Kalman filters approximate the nonlinearities of the system's dynamics by linearizing the system model around the current state estimate. [12] Although this paper provides promising results on developing more efficient tuning methods for Kalman filters, the critical issues, such as the possibilities of estimation errors introduced by the non-linearity, need for large computing capacity, and an accurate initialization etc., still persist. [13]

Unlike extended Kalman filters, unscented Kalman filters can implement non-linear systems, reducing estimation errors as a result. Several papers implement UKF for SOC and SOH estimation by propagating the battery system's state through a base nonlinear model, such as second-order resistance capacitance (RC) model, Thevenin model etc. [14], [15]. However, the effectiveness of the UKF model relies heavily on the underlying battery model with varying performance among different UKF implementations with different base models [15].

While model predictive control methods have shown promising results for Lithium-ion batteries, they still are not able to solve the issue of depending on an underlying base model. Model-based methods also rely on SOC and SOH references [16], further increasing the risk of estimation errors.

Data Driven Methods

This is the more recent method of SOC & SOH estimation. The data-driven method establishes nonlinear mapping characteristics between SOC and measured variables such as temperature, current, and voltage, and then makes predictions according to the given input. It achieves this by treating the battery as a black box and directly learning its internal dynamics through massive charge-discharge data [17].

A fuzzy logic-based SOC estimation framework is proposed in [18]. The Fuzzy logic (FL) framework makes adjustments to the gain factor added to the SOC estimation based on the error and changes in the actual SOC and the SOC estimated by Coulomb counting. The CC based SOC had an error due to the initial calibration based on the OCV-SOC curve and the error from the current sensor. The FL-based SOC estimation also has a negative effect because the FL table must be recalibrated every time there is a change in the cell's chemistry.

Artificial Neural Networks (ANNs) are pretty popular for real-time estimation – the most common architecture being the Feedforward Neural Network (FNN) [19]. For SOC estimation, it takes measurable signals such as current, voltage, and temperature as inputs and learns the nonlinear mapping to the SOC through one or more hidden layers. A drawback is that it struggles to adapt to unseen conditions like temperature variations or battery ageing, which limits its robustness in real-world use. Another is the Backpropagation Neural Network (BPNN) which improves the FNN by iteratively adjusts the connection weights based on gradient descent to improve SOC estimation accuracy. While it can achieve good performance with sufficient data, its main drawback is that it converges slowly and it susceptible to local minima. This makes it sensitive to initialization and training conditions.

The Recurrent Neural Network (RNN) retains information from previous time steps through internal memory loops, allowing it to capture the dynamic relationships between voltage, current, and temperature over time [19]. More advanced variants of the RNN are Long Short-Term Memory (LSTM) and Gated Recurrent Unit (GRU) which are effective as they can model these temporal dependencies in battery behavior.

More about LSTMs, GRUs and our method

A comparison between LSTM and GRU was conducted on EV battery data in [20]. The social estimation performed by the GRU architecture was better than that of the LSTM model, despite both models being trained with the same number of layers. The reduced complexity, resulting from the fewer gates in the GRU compared to LSTM, is another reason. Both models proposed in this work lack a physics-informed Loss function for the network. A physics-informed ensemble learning approach for the LSTM network had a better predictive capability in [21]. The ensemble learning framework had a leverage over the normal LSTM, both in terms of physical information utilization and model integration, resulting in better performance.

While most of the work involves either estimating SOC or estimating SOH, Zheng *et al.* proposed a joint estimation pipeline where the initial estimation is made to estimate the SOH to find the current capacity of the Battery with respect to the SOH, followed by a SOC estimation, making it a co-estimation pipeline with Support Vector Machine (SVM) based SOH estimation model and combined Computational Neural Network (CNN)-LSTM based network to predict the SOC, here the CNN model is used in feature extraction for SOC estimation [22].

Our work aims to implement a framework utilizing a GRU-PINN-based SOH estimation model and a GRU-PINN-based SOC estimation model in the pipeline. The proposed Framework is shown in Fig.2.

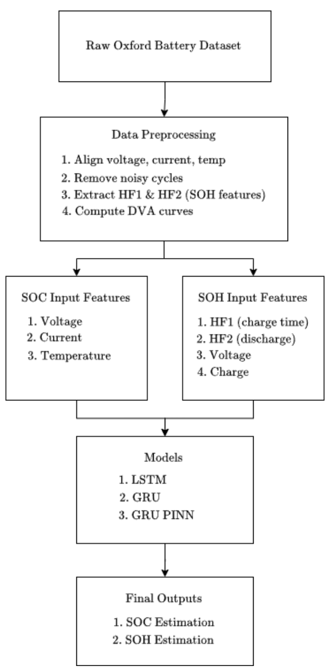

Figure 2. Physics Informed Estimation Pipeline

The 2-RC ECM as seen in [23] is taken as the baseline for defining the physics-based loss function for SOC estimation, making the network know the relationship between the OCV and the ECM model parameters with respect to the SOC of the battery and also defining the Differential voltage Analysis(DVA) based peaks to the loss function, like in [24] for the SOH estimation during the training process of the GRU network to make the PINN framework. Making our network rely on both these parameters for the loss function makes it easier to be deployed in actual hardware due to the fact that most of today's BMS algorithms are highly dependent on the ECM and do SOH estimation based on DVA.

Most studies on SOC and SOH estimation commonly use the NASA [25] and Oxford [26] battery datasets to train and validate their algorithms. Following this standard practice, we will also use the Oxford Battery Dataset. It provides voltage, current, temperature, and capacity measurements across multiple cells and degradation stages, allowing us to benchmark our model against existing methods.

3. Recurrent Neural Netwroks

A RNN works differently from a regular ANN in its approach to processing data. The data flow is from the input to the output, while in an RNN, it feeds information back into the network at each step. RNNs are designed to handle sequential data where they process inputs one step at a time while maintaining the hidden state that carries information from the previous step, which makes them suitable for time series prediction and modeling system dynamics. However, simple RNNs will suffer from the vanishing gradient problem.

The Long Short Term Memory (LSTM) and GRU are improved forms of RNN architectures designed to overcome the problem. LSTMs work by controlling how information flows through a sequence using three gates: a forget gate, an input gate, and an output gate. At each time step, the forget gate decides what past information should be erased, the input gate selects what new information should be stored, and the output gate determines what part of the internal memory should influence the current output. This gated mechanism allows the LSTM to maintain a long-term memory while avoiding the vanishing gradient problem, making it effective for tasks where patterns stretch over long time spans—such as tracking battery behavior across complete charge–discharge cycles.

The GRUs simplify LSTMs by combining the input gate and the forget gate into a single update gate and streamlining the output mechanism, making GRUs computationally efficient, performing similarly to LSTMs, and is useful in tasks where simplicity and faster training are beneficial. The update gate controls both how much past information to keep and how much new information to write, while the reset gate determines how strongly the model should mix new input with older memory. With fewer parameters and simpler structure, GRUs train faster, use less memory, and often perform similarly to or better than LSTMs, especially when data is limited or when real-time, resource-efficient inference is required—such as in embedded battery management systems.

Battery SOC and SOH cannot be estimated from a single measurement; they depend on how the battery has been subjected to various charging and discharging conditions, as well as the temperature at which it is cycled. RNNs like LSTM and GRU naturally model this kind of sequential behavior, making them a strong fit for the estimation problem. Since these networks are primarily data driven, they might generalize poorly outside the training domain. Including the physics of the Equivalent Circuit Model, along with the GRU network's loss function, could offer a strong, interpretable, and robust model. While existing PINNs rely on feedforward architectures, substituting them with the GRU yields a model that can capture the temporal dependencies related to battery degradation and charge-discharge behavior.

The proposed GRU architecture for SOC estimation incorporates battery physics, enforcing the Coulomb Counting equation, which describes the relationship between the SOC and the applied current. The equation used to extend the GRU framework to GRU - PINN is shown in 4.

$$\frac{d\,\mathrm{SOC}}{dt}(t) = -\frac{I(t)}{C_{\mathrm{nom}}} \tag{4}$$

Where $\mathrm{SOC}(t)$ is the state of charge at that time stamp, C_{nom} denotes the nominal capacity of the battery (typically given in Ampere-hours, Ah), and $I(t)$ is the battery current at that time stamp. If $I(t) > 0$, it denotes discharging, and if $I(t) < 0$, it denotes charging. In the GRU–PINN framework, this differential equation is applied in discrete form across time steps in each sequence. For two consecutive steps k and $k+1$, the ODE becomes as in 5.

$$\mathrm{SOC}_{k+1} - \mathrm{SOC}_k \approx \alpha I_k \tag{5}$$

The alpha parameter is a learnable physics parameter that absorbs timestep and capacity scaling.

$$L_{\mathrm{phys}} = \left(\mathrm{SOC}^{\mathrm{pred}}_{k+1} - \mathrm{SOC}^{\mathrm{pred}}_{k} - \alpha I_k\right)^2 \tag{6}$$

This term in 6 is combined with the data loss of the GRU, which learns to produce SOC predictions that are both data driven and balanced with battery physics, forming the GRU-PINN framework for SOC estimation.

For SOH estimation, the GRU-PINN architecture predicts the entire DVA curve in the form $\frac{dV}{dQ}$. The DVA curve changes with aging. The different DVA curves for a Li-ion cell cycle denote the electrochemical phase transitions occurring within the battery's active materials. Consider a DVA curve. A shift in peaks denotes LLI, a peak shift change indicates LAM, the appearance of new peaks denotes the formation of the Solid Electrolyte Interphase (SEI) layer, and a flattened curve indicates increased resistance due to aging. Fig 3. shows one of the DVA curves for cell 4 in the Oxford battery dataset.

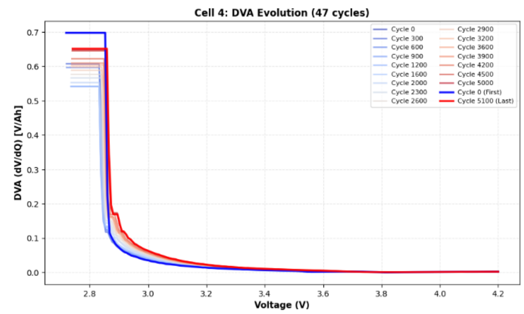

Figure 3. DVA Curve for cell 4

4. Methodology

The entire project is based on the Oxford battery dataset, which has the cell cycling data for 8 cells of 740 mAh capacity. The class was exposed to a constant current-constant voltage (CC-CV) profile. Three different networks, the LSTM, the GRU, and the GRU-PINN, were trained for SOC and SOH estimation. The cell, when charged and discharged for different numbers of cycles, shows a case of capacity fade, which denotes the change in the capacity of the cell when compared to the initial capacity, i.e., the SOH of the cell.

The features used to train the SOC estimation model are voltage, current, and temperature, as these are the only parameters that can be measured by the BMS, considering this is one of the networks that is going to be implemented in the actual Microcontroller (MCU), converting to an executable suitable for a certain MCU.Fig **??** shows the SOC of the cell with respect to time during charge. The SOC is increasing monotonically since the charge is done only at a constant C rate.

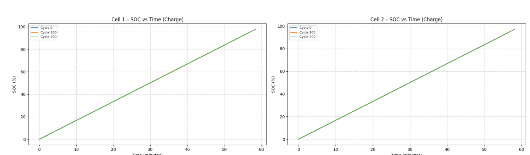

Figure 4. SOC vs time during charge

To estimate the SOH, two features, Health Feature 1 (HF1) and Health Feature 2 (HF2), along with the voltage and the charge accumulated in the cell as input parameters. During constant charging, the battery's charging current is stable while the voltage continuously increases. It is observed that as the number of cycles increases, the curve gradually shifts, indicating a shorter time for the battery to transition from low to high voltage. It denotes the decrease in battery capacity over time, which results in shorter charging times. But when considering an actual vehicle or a storage system, the battery does not start to charge from 0 and may not always be fully charged. HF1 is the constant voltage charging time, which ranges from 3.8V to 4.1V. HF2 extracts the feature as the constant voltage discharge time from 4.1V to 3.8V.

The correlation between HF1 and HF2 with respect to the SOH was found using Pearson's and Spearman's correlation coefficients. If the correlation value is close to 1, the correlation is strong, and if it is 0, the correlation is weak. The correlation matrices between these two features and the SOH are shown in Table 1.

Table 1. Correlation for HF1 and HF2 with SOH across all cells.

Cell	P_HF1	S_HF1	P_HF2	S_HF2
1	0.9992	1.0000	0.9802	0.9893
2	0.9960	0.9978	0.9483	0.9787
3	0.9994	0.9995	0.9871	0.9936
4	0.9977	0.9999	0.9873	0.9915
5	0.9986	0.9998	0.8609	0.9915
6	0.9955	0.9998	0.9651	0.9937
7	0.9988	0.9997	0.9918	0.9948
8	0.9987	0.9997	0.9839	0.9921

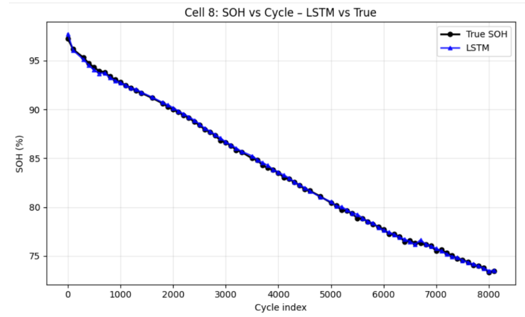

Figure 5. Estimated SOH for Cell 8 using LSTM

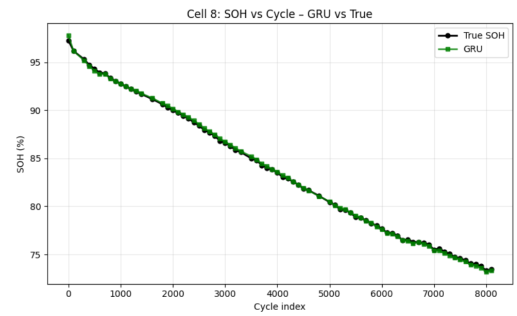

Figure 6. Estimated SOH for Cell 8 using GRU

4.1. SOH estimation

To perform the SOH estimation, the initial LSTM network is a 2-layer LSTM designed to predict SOH from time-series data with four features, including. charge, voltage, HF1, and HF2. The LSTM processes the sequence and learns temporal patterns to estimate the battery degradation. The network learns voltage-charge dynamics and health features evolve over time to estimate the remaining usable capacity of the battery. The charge and voltage were introduced as input features solely to facilitate the conversion to a GRU-PINN network in the future, as discussed in the RNN section. A similar 2-layer GRU model was designed to estimate the SOH from the same four features. Both models feature hidden units and dropout layers. The GRU and LSTM condense the whole cycle into a final hidden state, which is then fed into a linear layer to predict a single SOH value. AS discussed earlier, the GRU network outperformed the LSTM network. The estimated SOH based on both the LSTM and GRU networks is shown in Figure 5 and 7.

To extend the GRU network to a GRU-PINN network based on the DVA curve is formed by a two stage process. The model consists of the GRU network that processes sequential battery data. The GRU-PINN is initialized by loading the pre trained weights from the baseline GRU model from the GRU discussed before, which provides a strong baseline. The model is then fine-tuned using a combined loss function, the data loss, and the physics loss, which denotes the Mean Squared error between the predicted and true DVA curve. The total is denoted as in 7.

$$L = L_{\text{data}} + \lambda \frac{L_{\text{physics}}}{l} \tag{7}$$

where lambda is a weighting parameter denoting how much weight the DVA curve can have on predicting the SOH, and l is the length of the sequence, and is used to normalize. This constraint enables the model to learn physically meaningful representations of battery degradation, potentially improving generalization and interpretability compared to purely data-driven approaches. from the Fig 1 and the table 2. It is evident that the GRU-PINN did not perform as well as the GRU model. One reason could be that HF1 and HF2 are highly correlated with the SOH value, and the DVA curve may not properly interpret the physics involved.

Table 2. SOH prediction performance comparison of LSTM, GRU, and GRU-PINN models.

Model	MAE (%)	RMSE (%)	Max Error (%)
LSTM	0.142	0.183	0.513
GRU	0.127	0.154	0.539
GRU-PINN	0.193	0.234	0.710

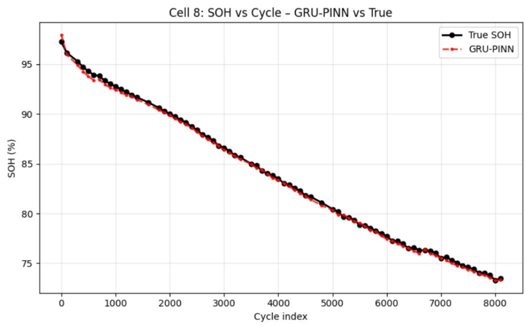

Figure 7. Estimated SOH for Cell 8 using GRU-PINN

4.2. SOC Estimation

To estimate the SOC of the cell in each and every cell cycle. The same three networks as the SOH estimation were compared. The number of parameters of the GRU and LSTM network used in both the models is shown Table 3.

Table 3. Model parameter comparison between LSTM and GRU.

Model	**Parameters**
LSTM	200,833
GRU	150,657
Difference	50,176 (33.3% more in LSTM)

From the metrics above, it is evident that the GRU model has comparatively fewer parameters and is lightweight, allowing it to be continuously implemented in an MCU. The physics-based loss function is also designed to be lightweight and less computationally intensive.

In the case of SOC estimation, there is a special case that requires consideration. Considering an actual vehicle or a Battery Energy storage the charging or the discharge process will not take place actually from 0% SOC to 100 % SOC or from 100 % SOC to 0% SOC. There is a high chance that the battery is charged or discharged in different SOC windows. The LSTM, GRU, and PINN networks were trained for the entire cycle and then tested on mid SOC windows. The result of the comparison is shown in Figures 8, 9 and 10.

It can be observed that the trained GRU-PINN-based SOC model yields a significant improvement over the LSTM and GRU models. This can also be verified using the table 4.

To make the model more efficient, the GRU-PINN model was trained using mid SOC windows. The result of the GRU-PINN model after training on the mid SOC is shown in Table 5.

Figures 11 and 12 show the estimation of mid-level SOC and the entire cycle during charging using GRU-PINN.It is observed from all the metrics and plots that the GRU-PINN-based SOC estimation performed better when compared to the LSTM and the GRU network. It can also be concluded that including battery physics along with the GRU network

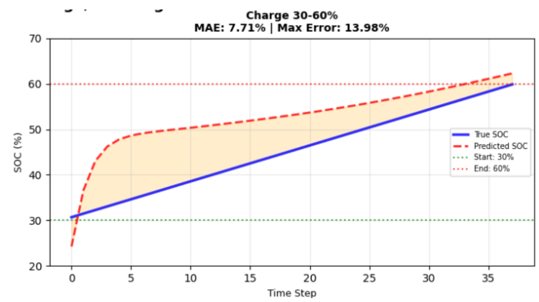

Figure 8. SOC estimation using LSTM network on Mid SOC

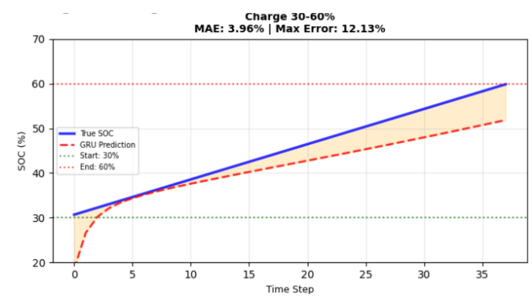

Figure 9. SOC estimation using GRU network on Mid SOC

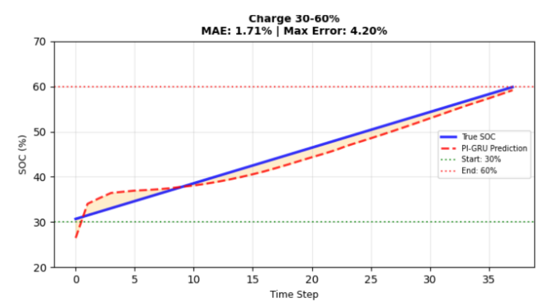

Figure 10. SOC estimation using GRU-PINN network on Mid SOC

Table 4. Overall validation metrics for LSTM, GRU, and GRU-PINN models.

Model	**MAE (%)**	**RMSE (%)**	**Max Error (%)**
LSTM	1.0550	1.4917	6.2685
GRU	0.5002	0.6682	2.4132
GRU-PINN	3.4621	4.1984	9.6410

Table 5. Validation metrics for GRU-PINN with augmentation.

Model	**MAE** (%)	**RMSE** (%)	**MaxErr** (%)
GRU-PINN with Augmentation.	0.1730	0.2194	1.0557

performs better for SOC estimation.

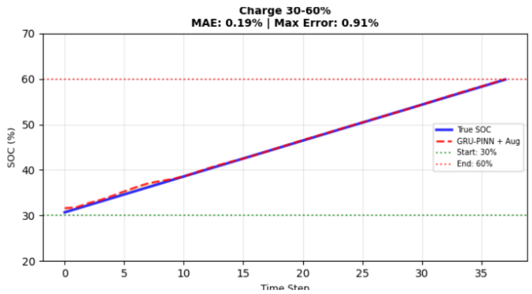

Figure 11. SOC estimation using GRU-PINN Augmented network on Mid SOC

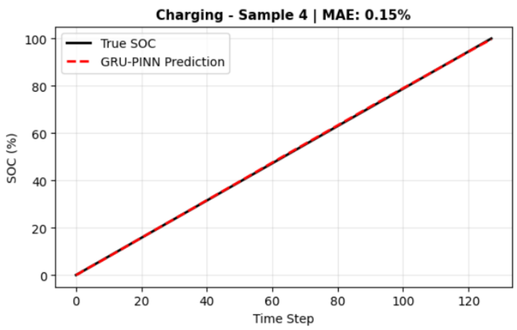

Figure 12. SOC estimation on the full charging cycle

When the models are implemented in actual BMS hardware, the input features may experience noise in the sensor readings. The sensor readings were simulated as Gaussian noise, and all three models' robustness to the noisy data was predicted.

The GRU-PINN model shows excellent robustness to voltage noise in SOH prediction. Only an 0.03% MAE increase is observed when noise level is increased from 0 to 0.2. The model is more robust than the GRU or LSTM, with GRU and LSTM providing much higher MAE.

For SOC prediction, the GRU model shows the most robustness, followed by the LSTM model. The GRU-PINN shows extreme drift compared to the other two, although this model outperforms the others for clean, noise-free data. With the largest degradation coming from voltage and temperature noise, the likely reason for this degradation is SOC's close coupling with open-circuit voltage.

5. Conclusion

This project implemented an idea on integrating the PINNs combined with the GRU for battery SOC and SOH estimation. Our analysis demonstrates that the GRU-PINN framework, incorporating the first order differential equation from Coloumb counting in the loss function, outperforms conventional GRU and LSTM models for SOC estimation. The physics-informed approach provided better accuracy and improved generalization to dynamic profiles, while remaining physically consistent across all SOC windows.

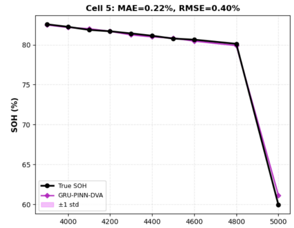

(a) GRU-PINN

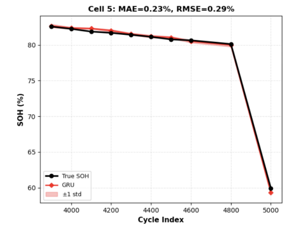

(b) GRU

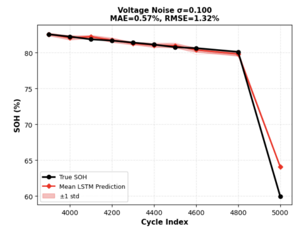

(c) LSTM

Figure 13. SOH estimation with noisy feature inputs for all three models: (a) GRU-PINN, (b) GRU, and (c) LSTM.

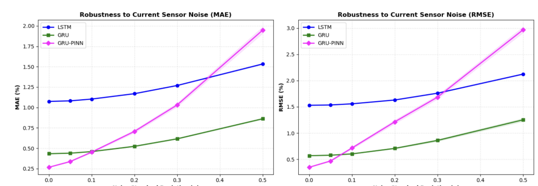

Figure 14. SOC prediction robustness to current sensor noise

However, our findings reveal that for SOH estimation, the standard GRU network without physics constraint performs comparably better than the GRU-PINN network. This suggests that the simple first-order differential equation we employed is insufficient to capture the complex degradation mechanisms governing battery health.

This work can be further improved by implementing the SOC estimation in Simulink for the actual cell with different vehicle drive cycles. We were unable to do that due to the lack of precise cell data in Simscape. It can also be improved by incorporating advanced electrochemical models (e.g., Single Particle Model, Doyle-Fuller-Newman model) that capture degradation mechanisms like SEI layer growth and lithium plating, and exploring hybrid approaches that combine data-driven capacity fade modeling with physics-based constraints on measurable variables.

References

[1] Kitalu Ricin Ngoy, Valantine Takwa Lukong, Kelvin O. Yoro, John Beya Makambo, Nonso Christopher Chukwuati, Chinedu Ibegbulam, Orevaoghene Eterigho-Ikelegbe, Kingsley Ukoba, and Tien Chien Jen. Lithium-ion batteries and the future of sustainable energy: A comprehensive review. *Renewable and Sustainable Energy Reviews*, 223:115971, 11 2025. 1

[2] Osman Demirci, Sezai Taskin, Erik Schaltz, and Burcu Acar Demirci. Review of battery state estimation methods for electric vehicles - part i: Soc estimation. *Journal of Energy Storage*, 87:111435, 5 2024. 1

[3] Xiaojun Li, David Jauernig, Mengzhu Gao, and Trevor Jones. Battery cloud with advanced algorithms. *IoT Enabled Multi-Energy Systems: From Isolated Energy Grids to Modern Interconnected Networks*, pages 111–136, 1 2023. 2

[4] Honggang Du, Guangchen Liu, Jianwei Zhang, Guizhen Tian, and Shengtie Wang. Soc estimation of lithium-ion batteries based on adaptive ukf. *2021 IEEE 4th International Conference on Renewable Energy and Power Engineering, REPE 2021*, pages 137–140, 2021. 2

[5] Carlo Taborelli and Simona Onori. State of charge estimation using extended kalman filters for battery management system. In *2014 IEEE International Electric Vehicle Conference (IEVC)*, pages 1–8, 2014. 2

[6] Nicolas Sockeel, Masood Shahverdi, and Michael Mazzola. Impact of the state of charge estimation on model predictive control performance in a plug-in hybrid electric vehicle accounting for equivalent fuel consumption and battery capacity fade. *ITEC 2019 - 2019 IEEE Transportation Electrification Conference and Expo*, 6 2019. 2

[7] Sabine Piller, Marion Perrin, and Andreas Jossen. Methods for state-of-charge determination and their applications. *Journal of Power Sources*, 96(1):113–120, 2001. Proceedings of the 22nd International Power Sources Symposium. 2

[8] Xiaoyu Li, Zhenpo Wang, Lei Zhang, Changfu Zou, and David D Dorrell. State-of-health estimation for li-ion batteries by combing the incremental capacity analysis method with grey relational analysis. *Journal of power sources*, 410:106–114, 2019. 3

[9] Nassim Noura, Loïc Boulon, and Samir Jemeï. A review of battery state of health estimation methods: Hybrid electric vehicle challenges. *World Electric Vehicle Journal*, 11:1–20, 12 2020. 3

[10] Gregory Plett. 2015. 3

[11] Kiarash Movassagh, Sheikh Arif Raihan, Balakumar Balasingam, and Krishna Pattipati. A critical look at coulomb counting towards improving the kalman filter based state of charge tracking algorithms in rechargeable batteries. 1 2021. 3

[12] M. Acquarone, F. Miretti, D. Misul, and S. Onori. Sleek dual extended kalman filter for battery state of charge and state of health estimation in electric vehicle applications. *SAE Technical Paper*, (2024-24-0023), 2024. 3

[13] Martin Murnane and Adel Ghazel. A closer look at state of charge (soc) and state of health (soh) estimation techniques for batteries. *Analog Devices Technical Articles*, 2023. 3

[14] Shulin Liu, Xia Dong, Xiaodong Yu, Xiaoqing Ren, Jinfeng Zhang, and Rui Zhu. A method for state of charge and state of health estimation of lithium-ion battery based on adaptive unscented kalman filter. *Energy Reports*, 8(Supplement 8):426–436, 2022. 3

[15] Shulin Liu, Xia Dong, Xiaodong Yu, Xiaoqing Ren, Jinfeng Zhang, and Rui Zhu. A method for state of charge and state of health estimation of lithium-ion battery based on adaptive unscented kalman filter. *Energy Reports*, 8:426–436, 2022. The 2022 International Conference on Energy Storage Technology and Power Systems. 3

[16] Changfu Zou, Chris Manzie, and Dragan Nešić. Model predictive control for lithium-ion battery optimal charging. *IEEE/ASME Transactions on Mechatronics*, 23(2):947–957, 2018. 3

[17] Zhansheng Ning, Zhongwei Deng, Jinwen Li, Hongao Liu, and Wenchao Guo. Co-estimation of state of charge and state of health for 48 v battery system based on cubature kalman filter and h-infinity. *Journal of Energy Storage*, 56:106052, 2022. 3

[18] Vishnu Jawaharram, E. Krishnan, K. Chandrakala, and Sampath Kumar. Adaptive soc estimation and improvised cell balancing techniques with iot-based scalable modular li-ion battery management system. *International Review of Automatic Control (IREACO)*, 17:175, 09 2024. 3

[19] Angelo Bonfitto. A method for the combined estimation of battery state of charge and state of health based on artificial neural networks. *Energies*, 13(10), 2020. 3

[20] Mouleshwar Saravanan, J. Ajaykumar, K. S. Arun, S. P. Sibhiecharan, and T. Ananthan. Lithium-ion battery soc prediction using deep learning. *2024 15th International Conference on Computing Communication and Networking Technologies, ICCCNT 2024*, 2024. 3

[21] Hanqing Yu, Zhengjie Zhang, Kaiyi Yang, Lisheng Zhang, Wentao Wang, Shichun Yang, Junfu Li, and Xinhua Liu. Physics-informed ensemble deep learning framework for improving state of charge estimation of lithium-ion batteries. *Journal of Energy Storage*, 73:108915, 12 2023. 4

[22] Minggang Zheng and Xing Luo. Joint estimation of state of charge (soc) and state of health (soh) for lithium ion batteries using support vector machine (svm), convolutional neural network (cnn) and long sort term memory network (lstm) models. *International Journal of Electrochemical Science*, 19:100747, 9 2024. 4

[23] Hafiz Muhammad Jawaad, Muhammad Saeed, Anjum Naeem Malik, Arash Khalatbarisoltani, Hassan Elahi, and Umar Shahbaz Khan. Physics-informed machine learning for state of charge estimation of lithium-ion batteries. *6th International Conference on Robotics and Automation in Industry, ICRAI 2024*, 2024. 4

[24] Fei Xia, Kangan Wang, and Jiajun Chen. State of health and remaining useful life prediction of lithium-ion batteries

based on a disturbance-free incremental capacity and differential voltage analysis method. *Journal of Energy Storage*, 64:107161, 8 2023. 4

[25] B. Saha and K. Goebel. Battery data set, nasa ames prognostics data repository. http://ti.arc.nasa.gov/project/prognostic-data-repository, 2007. Accessed via SCIRP ReferenceID = 3297577. 4

[26] J.M. Reniers, G. Mulder, and D.A. Howey. Oxford energy trading battery degradation dataset, 2020. Dataset accessed via Oxford University Research Archive. DOI: 10.5287/bodleian:gJPdDzvP4. 4